Vol. 29 (1998) *ACTA PHYSICA POLONICA B* No 1–2

# PHYSICS WITH POLARIZED PHOTONS AT SPring-8*

M. Fujiwara, T. Hotta, T. Kinashi, K. Takanashi, T. Nakano

Research Center for Nuclear Physics, Osaka University
Ibaraki, Osaka 567, Japan

Y. Ohashi, S. Daté, H. Ohkuma and N. Kumagai

Japan Synchrotron Radiation Research Institute, SPring-8
Kamigoori-cho, Ako-gun, Hyogo 678-12, Japan

*(Received November 24, 1997)*

We discuss physics opportunities at SPring-8 using GeV-photons and MeV-photons obtained by Compton backscattering of laser photons from 8 GeV electrons. We show a principle of Compton backscattering and an overview of applying a high energy photon beam for physics experiments. A new facility at SPring-8 is under construction, aiming at physics experiments using a polarized photon beam in the energy range of 1.5$\sim$3.5 GeV. The main subject is to study sub-nucleonic degree of freedom through the measurements of various produced mesons. In addition, we present a possibility of nuclear resonance fluorescence (NRF) experiments with high intensity polarized photons at several MeV energies with an intensity of $10^8 \sim 10^9$ per second.

PACS numbers: 13.60. Fz, 25.20. –x, 25.70. Ef

## 1. Introduction

As an extension of the RCNP physics program, we construct a new facility at SPring-8 [1], where a GeV photon beam in the energy range of $E_\gamma = 1.5\sim3.5$ GeV becomes available. The GeV photons are produced via Compton backscattering, and are used to study the sub-nucleonic structure of the nucleon. The key ingredients are the quarks — the building blocks of nucleons. The investigation of the fundamental role of quarks in nucleon or in a nucleus is the current topics in physics to reveal the underlying basic principle. The confinement mechanism of quarks and the microscopic

* Presented at the XXV Mazurian Lakes School of Physics, Piaski, Poland, August 27–September 6, 1997.

structure of mesons and excited nucleon in terms of quarks are the subjects to be understood in the program at SPring-8.

This project will offer an unique opportunity to study the quark system in a nucleon or in a nucleus by means of real polarized photons with the energy of 1.5∼3.5 GeV [2]. Using the Compton backscattered photons induced by a short-wave-length laser light, we generate the polarized multi-GeV photons. The high quality 8 GeV electron beam stored in the SPring-8 storage ring facility allows to provide such high energy photons.

Experiments with real photons are usually clean and powerful to study quark structures of nucleons, and offer definite information. This unique feature makes real-photon experiments complementary with electron-scattering experiments.

In addition to the high energy GeV photons, there is another possibility to generate a low energy MeV photon beam with an extremely high intensity. If a laser light in the infra-red wavelength region is applied for Compton backscattering, a high intensity $\gamma$ beam in the MeV energy region is available. Since the intensity of highly polarized $\gamma$ rays are inferred to amount to $\sim 10^9$ photon/second, the M1 and E1 resonances in nuclei can be very easily studied by the nuclear resonance fluorescence (NRF) method.

In this report, after explaining the photon beam characteristics at SPring-8, we show the overview of the physics with the polarized GeV photons and a possibility of the study of the M1 and E1 resonances with a high-intensity $\gamma$ ray beam.

## 2. GeV photon beam at SPring-8

A high energy $\gamma$ beam will be created by a method of Compton backscattering of a laser light from the electron beam at 8 GeV [3]. The SPring-8 storage ring can circulate the 8 GeV electron beam with a size less than 0.3 mm in diameter. Thanks to the relativistic effect with a very large Lorentz factor $\gamma$=16,000, Compton backscattered photons gain an energy of about $5\times10^7$ times higher than that of incident laser photons. The concept of the Compton backscattering is shown in Fig. 1.

The available energies of scattered photons are easily calculated by applying the four momentum conservation law for the initial 8 GeV electron and a laser photon. Let us first calculate the maximum $\gamma$ energy as a function of the laser energy. A schematic diagram of the Compton backscattering process is shown in Fig. 1. The energy relation between the energies of laser light and backscattered photons is easily derived using the conservation laws of energy and momentum. Momentum conservation gives

$$\vec{p_0} - \vec{\omega_0} = \vec{p_1} + \vec{\omega}. \tag{1}$$

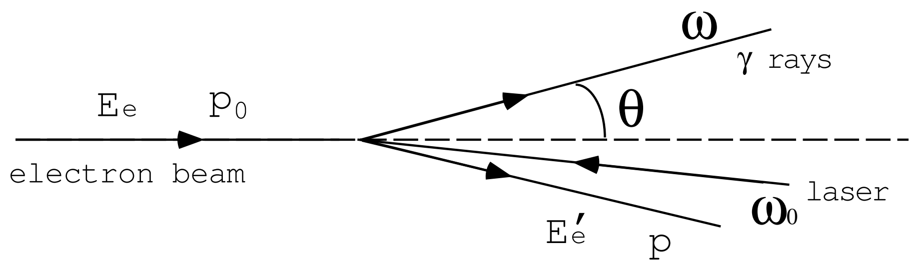


Fig. 1. Backscattered Compton Process via the collision between high energy electron and laser light.

Energy conservation is

$$\omega_0 + \sqrt{{p_0}^2 + m^2} = \omega + \sqrt{{p_1}^2 + m^2}. \tag{2}$$

Making the scaler product gives

$$\vec{p_0} \cdot \vec{\omega_0} = p_0\, \omega_0, \tag{3}$$

$$\vec{p_0} \cdot \vec{p_1} = p_0\, p_1 \cos\phi, \tag{4}$$

$$\vec{p_0} \cdot \vec{\omega} = p_0\, \omega, \tag{5}$$

$$\vec{\omega_0} \cdot \vec{\omega} = \omega_0\, \omega \cos\theta, \tag{6}$$

where $\phi$ is the angle between the incident and scattered electron momenta. The energy $\omega$ of the Compton backscattered photons is

$$\omega = E_\gamma = \frac{p_0\, \omega_0 + \omega_0 \sqrt{{p_0}^2 + m^2}}{\omega_0 + (\omega_0 - p_0) cos\theta + \sqrt{{p_0}^2 + m^2}}. \tag{7}$$

When the incident energy of the electron beam is extremely high, the recoiled photons are scattered in the backward direction ($\theta\approx 0$, $\phi\approx 0$, $m^2/{p_0}^2 \ll 1$). We obtain the following approximate relation:

$$\sqrt{{p_0}^2 + m^2} \sim p_0 \left(1 + \frac{1}{2}\frac{m^2}{p_0^2}\right), \tag{8}$$

$$p_0 \sim E_e. \tag{9}$$

Finally, the energy of the Compton backscattered photons is obtained as a function of the scattering angle $\theta$;

$$\omega = \frac{4\omega_0 E_e^2}{m^2 + 4\omega_0 E_e} \left( \frac{1}{1 + \left(\frac{E_e^2}{m^2 + 4\omega_0 E_e}\right) \theta^2} \right). \tag{10}$$

The energy of the scattered photon is proportional to $E_e^2$ and to the laser photon energy $\omega_0$, respectively.

Eq. (10) suggests that a short-wave laser light and a high-energy electron beam are necessary to produce the high-energy photon beam. The electron energy is the most important factor in getting high energy photons. For instance, using 351.1 nm ($\omega_0$=3.53 eV) argon laser, we can get photons with a maximum energy of 2.49 GeV from 8 GeV electrons. On the other hand, when the electron energy is low, the available photon energy becomes much lower. We can only obtain 0.3 GeV or 1.5 GeV photons from 2.5 or 6 GeV electrons, respectively.

Another advantage of the Compton backscattered photons is the polarization; a polarized photon beam is easily obtained using a linear- or circular-polarized laser-light. An unique experiment is possible to measure polarization observable's by using this advantage.

Recently, the faculty of engineering of Osaka University succeeded to develop a new crystal called cesium lithium boric-acid oxide (CLBO) [4]. This crystal was successfully used as a wave length shifter to convert a red laser light to an ultra violet one with a high efficiency. Further research and development are in progress. On the basis of these developments, a compact and high-power system of ultra-violet laser will be realized [5,6]. The future laser system will provide a light with a wave length shorter than 200 nm, which corresponds to the energy of 6 eV. If we combine the future laser system and the 8 GeV electron beam at SPring-8, the energy of a Compton backscattered photon will reach to 3.47 GeV.

We estimate the limit of the photon beam intensity to be $\sim 10^7$/sec. This upper limit comes from the technical restriction for the loss rate of the electron beam intensity in the 8 GeV electron storage ring at SPring-8. When we have $10^7$ Compton scattering per second, the loss rate of the stored electron beam becomes 10% over the period of 10 hours. Since other experiments run simultaneously at SPring-8, the permissible loss rate could be $\sim$10% for 10 hours. There is no limiting factor with respect to the laser light intensity itself. In future, installation of a high power laser may be possible if a photon beam with a higher intensity is required.

Angular dependences of the scattered photon beam are easily read in Eq. (10). When the electron energy is low, clear dependence of the $\gamma$ ray energy on its scattered angle makes the use of collimator as a good means to obtain a monochromatic beam. Unfortunately, this easy method is not applicable when the electron energy is high because all scattered photons concentrate within the narrow angular cone defined by the width of $\Gamma = \sqrt{(m^2 + 4\omega_0 E_e)/E_e^2}$ as shown in Fig. 2.

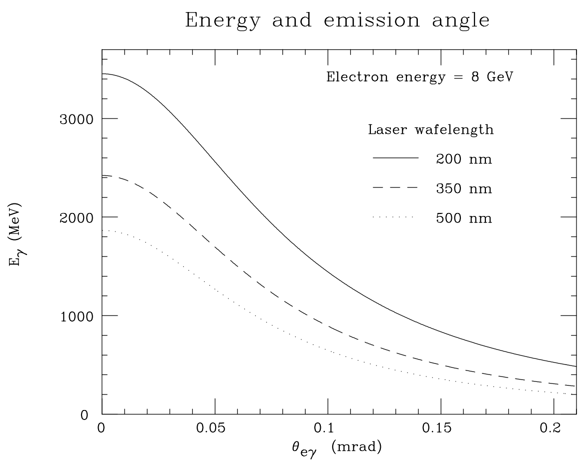


Fig. 2. Relation between Compton backscattered photons and its scattering angle. The $\gamma$ ray energies are plotted for laser light with the wave lengths of 200 nm, 350 nm and 500 nm. Higher the electron energy is, much more the scattered photons concentrate to forward direction(*i.e.* the direction of incident electron momentum. When the angle is large, the energy of photons slowly changes and it becomes independent on incident electron beam.

Scattered photons in the energy range between 1.5 and 3.5 GeV concentrate within $\Gamma \approx m/E_e = 0.063$ mrad even when the 6 eV ultra-violet laser-light and a 8 GeV electron beam make a head-on collision. Even if we install the target for an experiment at the point of 100 m downstream from the photon-electron collision region, the target size required could be less than 1 cm in diameter. As the photon beam concentrates in the extremely forward direction, the photon energy is not determined by means of a slit method in the case of the laser Compton backscattering with a high energy electron. In order to get information on the photon energy with an appreciable resolution, tagging of scattered electron energies is only a possible way.

Polarization is the unique feature of the Compton backscattered $\gamma$-rays. Fig. 3 shows the polarization property as a function of the $\gamma$ energy, which is reliably calculated from the QED theory.

The photon energy is determined by measuring the scattered electron momentum with position sensitive detectors (silicon strip detectors). A dipole magnet located at the downstream of the scattering region is used as a momentum analyzer. The energy resolution is estimated to be less than 30 MeV. Basic development of the system is in progress. Installation of the tagging system requires to modify some devices in the synchrotron radiation (SR) ring at SPring-8. We are currently constructing a new beam line with

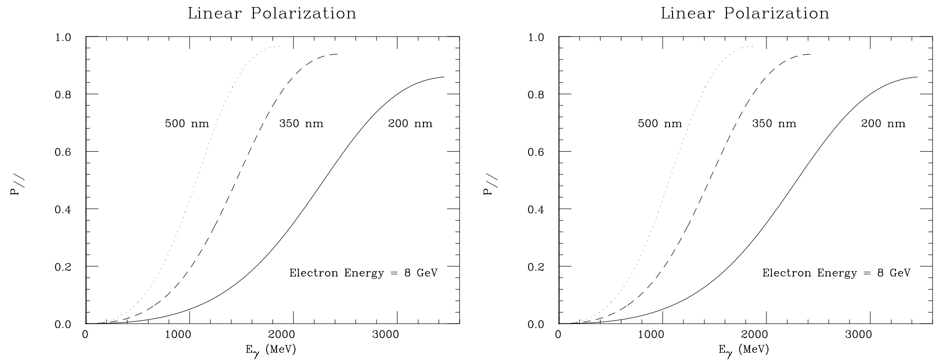


Fig. 3. Polarization of the backscattered photons induced by the 100% circular polarized laser light (left panel) and linear polarization of the backscattered photons induced by the 100% linear polarized laser light (right panel).

such the modifications. As the final remarks of this section, we compare the photon beam properties at SPring-8 with those at other facilities in the world as follows;

1. SPring-8, BNL, and ESRF are the photon factories which apply the method of the Compton backward scattering to generate high energy photon beams for nuclear physics experiments.

2. They store electrons in the storage ring at different energies ($E_\gamma$=8 GeV at SPring-8, 2.5 GeV at BNL and 6 GeV at ESRF). The electron beam energy of 8 GeV at SPring-8 is the highest one.

3. CEBAF is building extraction beam lines of 4 GeV electron beams for nuclear physics and a 3 GeV photon beam will be produced using by a bremsstrahlung method. The photon beam intensity is comparable with that at SPring-8. However, the background at forward angles is rather high in the experiment with the bremsstrahlung method.

4. Polarization of the photon beam at SPring-8 is higher than that at CEBAF.

In Table 2, we show the summary of the real photon experiments in the world. If we realized the SPring-8 facility, the energy region of the real-photon experiments in the range from 0.2 to 3.5 GeV is covered by three facilities at BNL, ESRF, and SPring-8.

TABLE I

Comparison of GeV photon beam properties

| Facility Energy (GeV) | Performance | Property |
|---|---|---|
| SPring-8<br>8 GeV | $E_\gamma$=3.5 GeV<br>I=$10^7$/sec<br>high polarization | backward Compton beam, Quark Nuclear Physics, high polarization experiments Hadron resonances, Hadrons in nuclei |
| BNL<br>2.5 GeV | $E_\gamma$=0.3 GeV | $\Delta$, $\pi$ excitations<br>backward Compton beam |
| ESRF<br>6 GeV | $E_\gamma$=1.5 GeV | Quark Nuclear Physics<br>backward Compton beam |
| CEBAF<br>4 GeV<br>(extraction beam) | $E_\gamma$=3 GeV<br>I=$10^7$/sec | bremsstrahlung beam<br>Quark Nuclear Physics, Hadron in nuclei |

## 3. Physics with GeV photons

A primary purpose of nuclear physics is to understand the internal structure of nucleons and a many-body system of nucleons. Atomic nuclei locate at the important hierarchy in nature in succession from the macroscopic world (cosmos) to the sub-nucleonic world with a Plank scale. A nucleon has a structure consisting of sub-nucleonic constituents, "quarks". Thus, the nucleon and the nucleus are believed to be well understood in terms of of the quarks and gluons, although the "nucleon and meson" picture works well in describing various nuclear phenomena.

Experimental information is still rare which is needed to test models in theories treating bound quark systems. Recent topics on the spin crisis is a typical one; what is the origin to carry the nucleon spin? What are the barion and meson structures? What happens when mesons and hadrons move in the nuclear medium? These are the major questions addressed. In this section, we present physics motivations to be explored in the experiments with a multi-GeV photon beam at SPring-8.

### *3.1. $s\bar{s}$ component of nucleon*

The constituent quark model predicts that the ratio ($\mu_n/\mu_p$) of the neutron and proton magnetic moments is $-2/3$, which agrees with the experimental value $-0.685$. This fact strongly supports the basic idea of "quark". However, the recent experiments from the lepton deep inelastic scattering address a serious question; the magnetic moments from constituent quarks only contribute 10%. The strange quarks give 10%$\sim$20% contributions [7,8].

The $\phi$ meson with the mass of 1020 MeV has the pure $s\overline{s}$ wave function. Thus, there is a possibility of pinning down $s\overline{s}$ components in a nucleon through the measurement of $\phi$ mesons produced via the knockout process. Polarization measurement is especially important since the asymmetry of the knockout processes would be sensitive to the helicity dependence.

Fig. 4 shows the important two cases of the $\phi$ meson production processes with $\gamma$ rays in the energy region of 1$\sim$3.5 GeV. One process is the pomeron exchange process, where a photon changes to a vector meson and is scattered from the multi-gluon exchange process (shown in Fig. 4a)). Since the pomeron has the same quantum number as vacuum, information on the nucleon spin is not carried out.

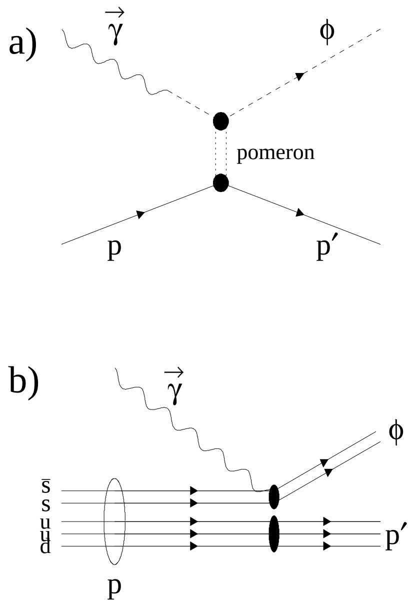


Fig. 4. Two photo-production processes of $\phi$ meson. a) Vector dominance process (VMD process). b) Knock-out process of $s\overline{s}$ pair by photons (knock-out process).

Fig. 4b) shows the knockout process, where the $s\overline{s}$ component is knocked out by a high energy photon. In this case, the knocked $s\overline{s}$ quark pair is the original ingredient of the nucleon, in addition to the $uud$ quark component. The $s\overline{s}$ pair carries information on the spin direction of nucleon together with the spin information of $uud$ quarks. The $s\overline{s}$ quark pair and the $uud$ quarks have to make the total nucleon spin 1/2 and the magnetic moments -0.685.

If the contribution of the knockout process in Fig. 4b) is experimentally checked, we can estimate the $s\overline{s}$ component in a nucleon. But, the situation is not easy. In the high energy region, the pomeron exchange process dominates. In the low energy region above the threshold of the $\phi$ production, the $s\bar{s}$ knockout process can compete the pomeron exchange process. Thus, the interference effect between the two processes in the energy region of 2$\sim$3.5 GeV becomes one of the most promising way to extract the information on the $s\bar{s}$ component.

At SPring-8, we plan to measure the interference effect between the pomeron exchange and knock-out process. Titov *et al.* [9] conclude that it is only possible to observe this interference effect in the photon experiment at 2$\sim$3.5 GeV. They conclude that the asymmetry observable is quite sensitive to the $s\bar{s}$ component.

### *3.2. Structure of baryons*

The baryon structures can be studied by means of a spectroscopic method to detect $\gamma$-rays and decay mesons from a baryon excited with a GeV photon beam. This is a remarkable way to reveal the wave function of a hadron consisting of quarks.

The shapes of excited nucleons and hyperons, and composite systems of quarks and gluons, could deform as nuclei do. The mass spectrum of baryons indicates that the nucleon deforms and rotates [10].

The excited states of nucleons are obtained in photo-absorption reactions. The measurements of radiative and mesonic decay will give a good means to get the structure information on the excited baryons which are clarified in terms of the QCD theories.

### *3.3. Gerasimov–Drell–Hearn sum rule*

The Gerasimov–Drell–Hearn (GDH) sum rule relates to the total photo-absorption cross sections by a polarized nucleon with the anomalous magnetic moment. A simple relation between the integrated photo-absorption cross section value and the magnetic moment of a nucleon is deduced by assuming fundamental principles such as the Laurentz and gauge invariance, causality, and unitarity [11,12,14]. The anomalous magnetic moment of the nucleon ($\kappa^2$) has a relation to the difference between the total cross sections with the nucleon spin parallel ($\sigma_{3/2}$) and anti-parallel ($\sigma_{1/2}$) to the circular polarized photons, integrated as a function of photon energy ($\nu$).

$$\int_0^\infty \frac{\sigma_{3/2} - \sigma_{1/2}}{\nu} d\nu = \frac{2\pi^2\alpha}{m^2}\kappa^2, \tag{11}$$

where $m$ stands for nucleon mass. This sum rule has never been tested because it requires measurements of absolute values of cross sections with a polarized photon beam on a polarized target. There are the approved experimental projects at ELSA ($0.5 \leq E_\gamma \leq 3$ GeV) and at Mainz ($140 \leq E_\gamma \leq 800$ MeV) [13]. However, at SPring-8, much precise measurements of the high energy contribution of the DGH sum rule is possible thanks to a high energy and high polarized photon beam.

The total photo-absorption cross sections at the energy range of 1.5∼3.5 GeV will provide a means of checking the QCD model [14,15]. Measurements at three facilities in different energy regions will be complementary to each other because the test of the sum rule and the QCD model requires the cross section data in the wide energy region.

The Compton scattering experiment from proton is complementary to the GDH experiment. Gell–Mann, Goldberger, and Thirring describe the Compton scattering between the polarized photon and polarized proton [16] and point out that the Compton scattering relates to the proton magnetic moment and the charge distribution of proton. Thus, if we can measure the Compton scattering at $1.5 \sim 3.5$ GeV, the experiment will provide detailed information on the microscopic structure of proton.

### *3.4. Structure of mesons*

The structures of mesons are still not well understood. Experimental studies are still required. Mesons are created by photo-absorption. They can be identified by reconstructing final state particles. Measurements of the branching ratio of radiative decays and polarization-observable's would be a key to understand mesonic structures. Knowledge on $q\overline{q}$ or glueball structures is important to understand physics of QCD. An axial vector particle (strong boson) with a mass of about 1.5 GeV and the QCD monopoles can be identified through these studies. The presence of these particles is a natural consequence in the scenario of the quark confinement caused by the QCD monopole condensation [17,18]. The observations of these new particles will reveal the quark confinement mechanism. Symmetry violations and fundamental principles in physics can be studied by measuring rare decays of $\eta$ and $K$ mesons.

### *3.5. Photo-disintegration of deuteron*

Photo-disintegration of a deuteron is a simplest reaction in which a deuteron is broken up into a proton and a neutron by photo-absorption. This reaction is important in order to understand the nucleon–nucleon interaction. Deuteron is essentially a two-nucleon system bound by the strong force. The study of the deuteron system has a long history. But, valuable information is still missing in the region above 1 GeV. One may see an interplay between the nucleon and quark aspects from the photo-breakup experiment on deuteron.

A transition from a meson picture to a quark picture will appear in the region between 1 and 3 GeV in order to understand the various observable's associating to deuteron. One may distinguish a marked difference between the nucleon- and quark- pictures via the polarization measurements with a polarized beam.

SPring-8 is an unique facility which provide the feasibility of the above-mentioned experiments with a high quality $\gamma$ beam of the energy range between 1.5 and 3 GeV.

### *3.6. Hypernuclei*

A Multi-GeV photon beam creates strangeness-nuclei (hyper-nuclei) via the ($\gamma$,K) reactions. The ($\gamma$,K) reactions are complementary to the ($\pi$,K) and (K,$\pi$) reactions. A polarized photon beam is used for production of hyper-nuclei. Information on flavor changing weak interaction in nuclei is obtained via the measurement of weak decays of hyper-nuclei. They shed a light on clues for studying chiral symmetry breaking and the quark and gluon confinement mechanism in nuclei.

### *3.7. Physics with vector mesons*

Vector mesons of $\rho(770)$, $\omega(782)$ and $\phi(1020)$ couple strongly to photons in the nuclear medium. The vector dominance model predicts that the vector mesons are created with the same helicity with that of incident photons. The validity of the vector dominance model has been checked for $\rho(770)$ only within the accuracy of 10%. This validity should be examined for $\omega(782)$ and $\phi(1020)$ with a high accuracy at high energies.

Theorists predict a decrease of the mass of vector mesons in the nuclear medium. This mass reduction is due to the partial restoration of the chiral symmetry breaking in nuclear environments with a high nucleon-density [19, 20]. It is still not known whether the vector mesons, $\rho(770)$ and $\omega(782)$, become heavier or lighter in dependence on the nuclear matter density and on the nuclear temperature [21, 22].

Photo production of vector mesons is possible at SPring-8. The mass of the produced vector meson is measured by reconstructing the invariant mass of the decay particles. At present, such mass measurements are tried via the hadron-hadron and heavy ion collisions. But, in the case of hadron-hadron and heavy ion collisions, the impact parameter is not well defined. Thus, it would be very difficult to experimentally determine the nuclear matter density at the position of the vector meson production. If the density dependence of the mass change is very small, the precise mass-change measurements would be required and are generally difficult. In the photoproduction, the advantage is that the density is those obtained from the electron scattering, and that the incident channel and outgoing channel are theoretically predictable if we measure the lepton-pair from the decay of the vector meson. If the meson production process has a strong dependence on the nucleon spin, it is possible that the directional change of the mass of the vector meson happens inside of the nucleon. This is called as the transverse and longitudinal mass changes. The angular correlation measurement of decay particles from the vector meson is promising to determine the polarization of the vector meson in a nucleus, through which one may see the directional difference of the mass change.

## 4. Nuclear Resonance Fluorescence at SPring-8

### *4.1. Advantage at SPring-8*

The 8 GeV storage ring at SPring-8 is used mainly as a synchrotron radiation light source. However, it can be also used for nuclear physics purpose as a source of $\gamma$ rays. The low-energy photon production from the Compton backscattering (CBS) has two advantages. The energy spectrum of the $\gamma$ rays consists of much more high energy photons than for the Bremsstrahlung method. Additionally, the resulting photons are naturally polarized, up to 100%, depending on the scattering angle in the c.m. system of photon and electron.

Because there is no loss of electron number in the storage ring, experiments can be performed parasitically, independent of other experiments. Also, the power needed to accelerate the struck electron to the mean beam energy is negligible (*e.g.*, to accelerate $10^{10}$ electrons per second by 10 MeV one needs 0.16 W). The radio frequency (RF) cavities for acceleration are working at a frequency of 508.58 MHz, thus the beam is nearly continuous with a bunch separation time of $\sim$2 ns.

If the laser light were backscattered to the electron beam direction, the photon maximum energy becomes

$$\omega_{\max} = \frac{4\omega_0 E_e^2}{m^2 + 4\omega_0 E_e}. \tag{12}$$

Table II lists the available energy of the Compton backscattered photons. To produce $\gamma$ rays with a few MeV for Nuclear Resonance Fluorescence (NRF) experiments, lasers with wavelengths of the order of a few 100 $\mu$m are needed. It seems to be rather difficult to obtain such a laser system for the light of a few 100 $\mu$m. This is a dis-advantage. But, if such a laser light were realized with the intensity of about 1W [23], we can get a high intensity

MeV $\gamma$ rays from the 8 GeV electron beam. For example, the photon energy of the 120 $\mu$m laser light is 0.0103 eV, and those of the 240 $\mu$m laser light is 0.00517 eV. When we irradiate these laser lights to the 8 GeV electron beam, we can get the maximum $\gamma$ energy of 10.11 MeV and 5.07 MeV. The Compton backscattered photons is focused within $\Gamma \approx m/E_e = 0.063$ mrad. This means that the emission angle of photons are almost determined by the divergence angle of the 8 GeV electron beam at the collision point.

TABLE II

Energy of Compton backscattered photons from 8 GeV electrons. It is worthy noting that the infra-red laser beam contains much more photons if we use the same power laser. The notations $\lambda$, $\omega_0$, $\omega$ and $\Gamma$ stand for the laser wavelength, the laser photon energy, the maximum energy of the Compton backscattered photon, and the half width of the scattered angle, respectively. The last column shows the photon intensity included in the 1 Watt laser.

| $\lambda$ | $\omega_0$ | $\omega$ | $\Gamma$ (mrad.) | $I$(photons/sec)/Watt |
|---|---|---|---|---|
| 200 nm | 6.20 eV | 3450 MeV | 0.085 | $1\times10^{18}$ |
| 350 nm | 3.54 eV | 2421 MeV | 0.076 | $1.76\times10^{18}$ |
| 500 nm | 2.48 eV | 1860 MeV | 0.073 | $2.52\times10^{18}$ |
| ... | ... | ... | ... | ... |
| 120 $\mu$m | 0.0103 eV | 10.11 MeV | 0.068 | $6.06\times10^{20}$ |
| 240 $\mu$m | 0.00517 eV | 5.07 MeV | 0.066 | $1.21\times10^{21}$ |

Since the photon energy of the laser light is extremely low, the laser beam contains a huge number of the quantum photons compared with the case of the ultra violet laser (more than a factor of 100!). Since the energy loss of the recoiled 8 GeV electron is very small, the recoiled electron can again circulate in the storage ring. This means that we can irradiate the 8 GeV beam with a higher intensity laser light. There is a possibility for us to easily obtain the $\gamma$ intensity of more than $10^9$/sec. If we install the laser system at the inside of the storage ring and make the laser cavity at the laser-electron collision point, the collision with the laser light will be increased by a factor of $10^6$ because that the laser cavity stores a huge number of photons.

### *4.2. M1 and E1 excitations*

Fig. 5 shows the excitation and decay processes of a nucleus. The nucleus is first excited by a photon. The excited level decays by $\gamma$ emission into the low-lying levels. In the past, using this process called "nuclear resonance fluorescence", many important experiments were carried out to study the levels excited via the magnetic and electric transitions [24,25]. Recently, the

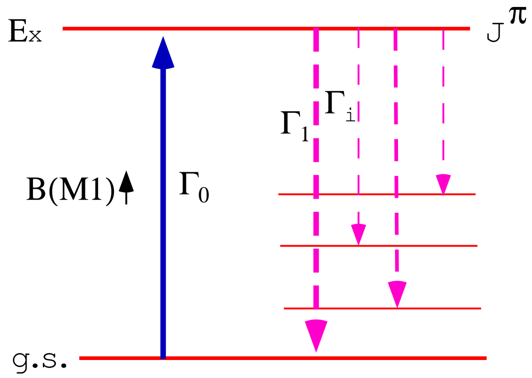


Fig. 5. Excitation and decay diagram of excited levels in a nucleus.

NRF method are used to investigate the nuclear scissors mode [26,27], which is one of the important collective motions of nuclei. Thus, the promising extension of the NRF experiment at SPring-8 is noteworthy.

Let us consider the $\gamma$ ray detection ratio from the NFR experiment at SPring-8. We examine the case of the M1 excitation. The full width of the decay process is the sum of all possible decay widths. The width and the excitation strength are related by

$$\Gamma_i = 8\pi \sum \frac{L+1}{L((2L+1)!!)^2} \left(\frac{E_0 - E_i}{\hbar c}\right)^{2L+1} \left(\frac{2J_0+1}{2J_i+1}\right) B(\pi L)\uparrow. \tag{13}$$

The absorption cross section is related to the width $\Gamma_0$ as,

$$I_{\mathrm{abs}} = \pi^2 \left(\frac{2J+1}{2J_0+1}\right) \left(\frac{\hbar c}{E_x}\right)^2 \Gamma_0. \tag{14}$$

In the case of the M1 excitation from the $0^+$ state to the $1^+$ state, the width can be written in a more simple way using the transition matrix $B(\mathrm{M1})$ as

$$\Gamma_0(0^+ \to 1^+) = 8\pi \, \frac{2}{9} \left(\frac{E_x}{\hbar c}\right)^3 \frac{1}{3} \, B(M1)\uparrow, \tag{15}$$

$$\frac{\Gamma_0}{(0^+ \to 1^+)\mathrm{meV}} = 3.8 \left(\frac{E_x}{\mathrm{MeV}}\right)^3 \frac{B(M1)\uparrow}{\mu_N^2}. \tag{16}$$

Since the nuclear magneton $\mu_N^2$ has a relation of $\mu_N^2 = 0.011 e^2\,\mathrm{fm}^2$, we get the following equation,

$$\frac{I_{\mathrm{abs}}(0^+ \to 1^+)}{\mathrm{MeV\,fm}^2} = 1.2 \times 10^{-3} \left(\frac{\mathrm{MeV}}{E_x}\right)^2 \frac{\Gamma_0(0^+ \to 1^+)}{\mathrm{meV}} \tag{17}$$

For an M1 excitation with an excitation energy of about 3 MeV, an strength of about 1 $\mu_N^2$, and the decay width $\Gamma_0$ of 0.1 meV, one gets $I_{\rm abs}$ of about 0.013 MeV fm$^2$. Assuming a target density of $10^{22}$/cm$^2$ (*e.g.*, 200 mg of $^{12}$C) and a photon flux of $10^8$/(5 MeV)/second, one gets a counting for that certain excitation of about 26 Hz into the full solid angle of $4\pi$. If we use a $\gamma$ ray detector with an efficiency of 2%, we can accumulate the total counts of about 45,000 for one level.

The recent development of the Ge detector is impressive. The large Ge detectors with the Compton suppressor of BGO scintillator are commercial. Combining these new Ge detectors with the high intensity MeV polarized photons, the precise mapping of the M1 and E1 excitation of nuclei is realistic.

Recently, a new possibility is suggested by Litvinenko *et al.,* [28]; a monochromatic $\gamma$ beam of ~12 MeV has been produced via Compton backscattering between the 500 MeV electrons and free-electron laser photons. They claim that the intensity of 100% linearly polarized $\gamma$ rays will amount to $10^9$–$10^{10}$ per sec.

We thank Professors H. Ejiri and H. Kamitsubo for their encouragement during the development of the BL33B2 course at the SPring-8 facility, where a new facility called “Laser-Electron-Photon” facility will be installed for nuclear physics developments under the mutual effort of SPring-8 and RCNP. This work was supported in part by the Ministry of Education, Science, Sports and Culture (Monbusho) with grant numbers of 09041108 and 07404012. We are grateful to acknowledge the support of the Science Technology Agency (STA). The authors acknowledge Dr. M. Kuss for estimating the $\gamma$ ray yields from NRF experiments during his stay as a STA fellow.

## REFERENCES

[1] H. Kamitsubo, in Proceedings of FRONTIER96, edited by H. Toki, T. Kishimoto and M. Fujiwara, World Scientific, March 7–9, 1996, p. 147.

[2] M. Fujiwara, T. Kinashi, T. Hotta, Journal of the Japanese Society for Synchrotron Radiation Research **10**, 23 (1997) (in Japanese).

[3] For historical papers: E. Feenberg, H. Primakoff, *Phys. Rev.* **73**, 449 (1948); R.H. Milburn, *Phys. Rev. Lett.* **10**, 75 (1969); F.R. Arutyunian, V.A. Tumanian, *Phys. Lett.* **4**, 176 (1963); J. Ballam *et al., Phys. Rev. Lett.* **23**, 498 (1969).

[4] Y. Mori *et al.*, *Appl. Phys. Lett.* **67**, 1818 (1994).

[5] S.C. Tidwell, J.F. Seamans, D.D. Lowenthal, G. Matone, G. Giordano, *Opt. Lett.* **18**, 1517 (1993).

[6] G. Giordano, G. Matone, *Nuovo Cim.* **12**, 927 (1990).

[7] EMC Collaboration, J. Ashman *et al.*, *Phys. Lett.* **B206**, 364 (1988).
[8] SMC, D. Adams *et al.*, *Phys. Lett.* **B329**, 399 (1994).
[9] A.I. Titov, Y. Oh, S.N. Yang, *Phys. Rev. Lett.* **79**, 1634 (1997).
[10] H. Fujimura, H. Toki, H. Ejiri, in Proceedings of FRONTIER96, edited by H. Toki, T. Kishimoto, M. Fujiwara, World Scientific, March 7–9, 1996, pp. 110.
[11] S.B. Gerasimov, *Sov. J. Nucl. Phys.* **2**, 430 (1966).
[12] S.D. Drell, A.C. Hearn, *Phys. Rev. Lett.* **16**, 908 (1966).
[13] G. Anton, *Prog. Part. Nucl. Phys.* **34**, 173 (1995).
[14] D. Drechsel, *Prog. Part. Nucl. Phys.* **34**, 181 (1995).
[15] A.M. Sandorfi, in Proceedings of FRONTIER96, edited by H. Toki, T. Kishimoto and M. Fujiwara, World Scientific, March 7–9, 1996, p. 17.
[16] M. Gell–Mann, M. Goldberger, W. Thirring, *Phys. Rev.* **96**, 1612 (1954).
[17] H. Toki, H. Suganuma, private communication.
[18] H. Suganuma, S. Sasaki, H. Toki, *Nucl. Phys.* **B435**, 207 (1995).
[19] T. Hatsuda, T. Kunihiro, *Phys. Rev. Lett.* **55**, 158 (1985).
[20] G.E. Brown, *Nucl. Phys.* **A488**, 689 (1988).
[21] T. Hatsuda *et al.*, *Nucl. Phys.* **B394**, 221 (1993).
[22] T. Hatsuda, S.H. Lee, *Phys. Rev. Lett.* **46**, R34 (1992).
[23] M. Rosenbluh, R.J. Temkin, K.J. Button, *Appl. Opt.* **15**, 2635 (1976).
[24] U.E.P. Berg, U. Kneissl, *Annu. Rev. Nucl. Part. Sci.* **37**, 33–69 (1987).
[25] A. Richter, *Prog. Part. Nucl. Phys.* **34**, 261 (1995).
[26] P. von Brentano, A. Zilges, R.-D. Herzberg, U. Kneissl, J. Margraf, H.H. Pitz, *Nucl. Phys.* **A577**, 191c (1994).
[27] P. von Brentano, *et al., Phys. Rev. Lett.* **76**, 2029 (1996).
[28] V.N. Litvinenko, *et al.* , *Phys. Rev. Lett.* **78**, 4569 (1997).